ACS APPLIED MATERIALS & INTERFACES

Research Article

www.acsami.org

Nonplanar Conductive Surfaces via "Bottom-Up" Nanostructured Gold Coating

T. P. Vinod and Raz Jelinek*

Ilse Katz Institute for Nanoscale Science and Technology and Department of Chemistry, Ben Gurion University of the Negev, Beer Sheva 8410, Israel

Supporting Information

ABSTRACT: Development of technologies for the construction of bent, curved, and flexible conductive surfaces is among the most important albeit challenging goals in the promising field of "flexible electronics". We present a generic solution-based "bottom-up" approach for assembling conductive gold nanostructured layers on nonplanar polymer surfaces. The simple two-step experimental scheme is based upon incubation of an amine-displaying polymer [the abundantly used poly(dimethylsiloxane) (PDMS), selected here as a proof of concept] with $Au(SCN)_4^-$, followed by a brief treatment with a conductive polymer [poly(3,4-thylenedioxythiophene)/poly(styrenesulfonate)] solution. Importantly, no reducing agent is co-added to the gold complex solution. The resultant surfaces are conductive and exhibit a unique "nanoribbon" gold morphology. The scheme yields conductive layers upon PDMS in varied configurations: planar, "wrinkled", and mechanically bent surfaces. The technology is simple, inexpensive, and easy to implement for varied polymer surfaces (and other substances), opening the way for practical applications in flexible electronics and related fields.

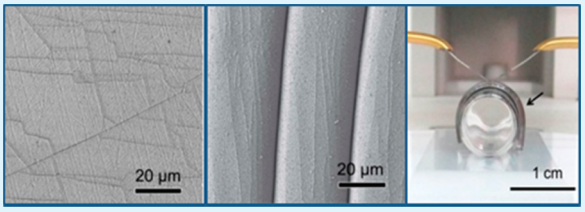

KEYWORDS: *poly(dimethylsiloxane) (PDMS), conductive gold films, Au nanostructures, bottom-up synthesis, flexible electronics*

INTRODUCTION

"Flexible electronics" is one of the most promising "new frontiers" in materials science, exhibiting broad potential for varied applications in publishing, electro-optics, solar energy, and others.[1−4] Research in this field focuses upon technologies that allow the fabrication of films and coatings exhibiting effective charge transport even while they are deposited on curved or bent objects.[5,6] Parallel efforts aim to construct surfaces that retain conductivity even after mechanical deformation (i.e., bending or stretching).[5,7] Conventional silicon-based surfaces, predominant in current micro-electronics, are generally rigid and thus constrained for the creation of three-dimensional and flexible conductive surfaces. Polymers, on the other hand, constitute excellent candidates for the fabrication of curved, flexible, and stretchable substrates for conductive surfaces.

Conventional, industrially applied metal deposition and patterning of conductive surfaces are almost exclusively carried out via "top-down" technologies, such as vapor deposition and lithography. These techniques face increasing challenges in terms of spatial flexibility, cost, and adverse environmental effects. Specifically in the context of nonplanar coatings, top-down techniques often result in inadequate film uniformity.[8] "Bottom-up" strategies relying on molecular self-assembly have recently emerged as viable alternatives for the construction of conductive surfaces, providing simple, inexpensive, and environmentally benign solution-based synthetic routes.[9−11] Expanding bottom-up technologies to the fabrication of conductive films on three-dimensional surfaces, however, is a formidable task, posing significant technical challenges.

We present a generic, simple strategy for fabricating nonplanar conductive surfaces. The approach combines spontaneous assembly of nanostructured gold layers through incubation of $Au(SCN)_4^-$ with an amine-displaying polymer surface,[12,13] followed by treatment with a conductive poly(3,4-thylenedioxythiophene)/poly(styrenesulfonate) (PEDOT/PSS) polymer mixture. We show that the new scheme facilitates the formation of conductive surfaces even upon "wrinkled" or mechanically bent polymer substrates.

EXPERIMENTAL SECTION

Materials. $HAuCl_4 \cdot 3H_2O$, KSCN, PEDOT/PSS (1.3 wt % dispersion in H_2O, conductive grade), and (3-aminopropyl)-triethoxysilane were purchased from Sigma-Aldrich and used as received. The Sylgard 184 kit (including monomer and curing agent) was purchased from Dow Corning. Water used in the experiments was doubly purified by a Barnstead D7382 water purification system (Barnstead Thermolyne, Dubuque, IA), at 18.3 mΩ cm resistivity.

Preparation of PDMS and Wrinkled PDMS. Planar PDMS samples were prepared using the instructions provided by the supplier. The monomer and curing agent were mixed in a 10:1 ratio and cured at 70 °C for 2 h on a hydrophobic surface. After being cured, samples were peeled off from the supporting surface. Wrinkled PDMS was made using a reported procedure.[14] Briefly, PDMS films were initially

Received: November 25, 2013
Accepted: February 19, 2014
Published: February 19, 2014

 © 2014 American Chemical Society

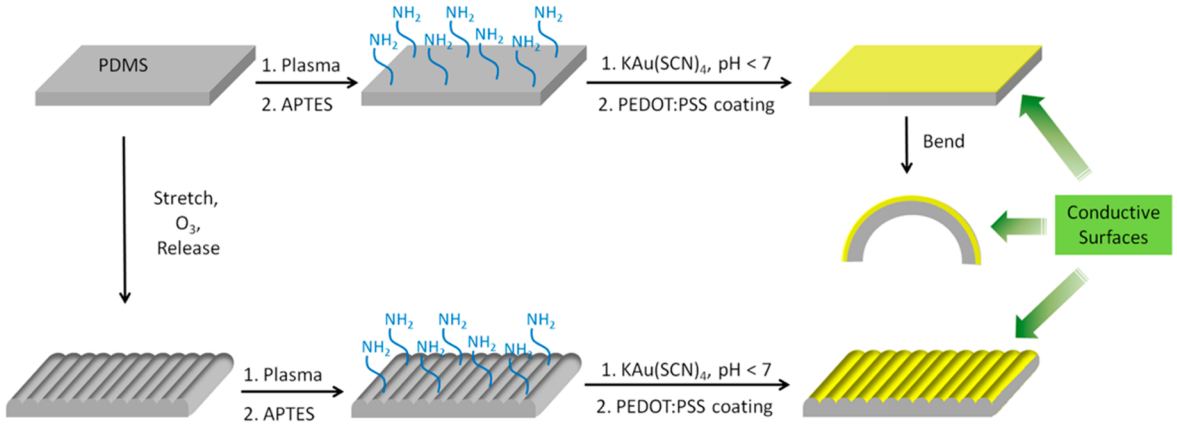

Figure 1. Fabrication of nonplanar conductive PDMS surfaces. Schematic illustration (not to scale) of two routes for assembly of nanostructured conductive Au films on a PDMS surface. In the top route, the gold layer is grown on a flat PDMS substrate through incubation of $Au(SCN)_4^-$ with amine-functionalized PDMS, followed by treatment with a PEDOT/PSS solution. The coated PDMS slab can be bent and still retains conductivity. The bottom route shows the physical deformation of PDMS, creating a wrinkled surface that is subsequently coated with gold through the same chemical procedure as the planar substrate.

prepared by mixing the elastomer and curing agent in a 20:1 ratio. These PDMS films were then mechanically pulled with uniaxial strain in a custom-made device (see Figure S1 of the Supporting Information for details) and kept in an ultraviolet−ozone (UVO) oven for 40 min. Wrinkles were produced on the PDMS surface after the strain had been released.

Amine Modification of the PDMS Surfaces. The PDMS surfaces were first treated in plasma for 3 min and subsequently immersed in a solution containing ethanol, water, and APTES in a 200:20:1 (v/v/v) ratio for 2 h.[15] Following this treatment, the substrates were washed consecutively with ethanol and water and then dried in a flow of compressed air.

Synthesis of the $KAu(SCN)_4$ Complex. Synthesis was based upon a published protocol.[13] Briefly, 1 mL of an aqueous solution of $HAuCl_4{\cdot}3H_2O$ (24 mg/mL) was added to 1 mL of a solution of KSCN in water (60 mg/mL). The precipitate formed was separated by centrifugation at 4000*g* for 10 min. The supernatant was decanted, and the residue was dried at room temperature.

Growth of Au Films on PDMS Substrates. The same procedure was used for gold film formation upon both the planar and wrinkled PDMS surfaces. An aqueous solution of $Au(SCN)_4^-$ (0.7 mg/mL) was prepared in water. The doubly distilled water used was adjusted to a pH of 5.5 by adding appropriate amounts of 0.1 M HCl prior to the solution preparation. The amine-modified PDMS substrates were vertically immersed in the solution and kept at 4 °C for 3 days. After the gold growth had reached completion, the substrates were taken out of the growth solution and washed thoroughly with water to remove unreacted materials and subsequently dried at room temperature.

PEDOT/PSS Coating. Au/PDMS samples were treated in plasma for 40 s to ensure complete reduction of the gold layer; 50 μL of a 1:2 (v/v) PEDOT/PSS disperion in 2-propanol was then dropped over the substrate and spin-coated for 1 min at 1000 rpm.

Instruments and Characterization. Scanning electron microscopy (SEM) and energy dispersive spectroscopy (EDS) were conducted with a JEOL (Tokyo, Japan) model JSM-7400F scanning electron microscope equipped with EDS (Thermo Scientific). Powder X-ray diffraction (XRD) measurements taken using a Panalytical Empyrean powder diffractometer equipped with a parabolic mirror on the incident beam providing quasi-monochromatic Cu Kα radiation (λ = 1.54059 Å) and an X'Celerator linear detector. X-ray photoelectron spectroscopy (XPS) analysis was conducted using a Thermo Fisher ESCALAB 250 instrument with a basic pressure of 2×10^{-9} mbar. The samples were irradiated in two different areas using monochromatic Al Kα, 1486.6 eV X-rays, using a beam size of 500 μm. Plasma treatment was conducted in a Harrick Plasma PDC-32G plasma cleaner. UVO treatment was conducted using a UVOCS T10X10/OES/E ultraviolet ozone cleaning system. AFM analysis was conducted with a Dimension 3100 SPM instrument from Digital Instruments (Veeco, NY). Electrical measurements were performed on a Keithley 2400 sourcemeter in a two-probe configuration. For the sample preparation of electrical measurements, the substrate containing the gold film was mounted in a thermal evaporator with a stainless steel shadow mask attached. Cr (10 nm) and Au (90 nm) were evaporated onto the substrates to obtain the electrode patches at a predefined spacing.

RESULTS AND DISCUSSION

Figure 1 depicts the experimental approach. To demonstrate the new technology, we have used a poly(dimethylsiloxane) (PDMS) substrate, as this easily deformed elastomeric organosilicon polymer is used in numerous and diverse commercial applications.[16,17] PDMS has been employed in particular as a substance for electrically conductive layers, platforms for electrodes in cyclic voltammetry, and other electronic applications.[18−20] In particular, patterned and intricate metal films were reported on a deformed PDMS surface through a combination of thermal expansion and vapor deposition.[21] As shown in Figure 1, two generic experimental schemes were examined, starting from a planar PDMS surface (top left). The reaction pathways in both routes were based upon a recently developed single-step process for assembly of nanostructured Au films through incubation of gold thiocyanate [$Au(SCN)_4^-$] with amine-displaying surfaces, without co-addition of reducing agents.[12,13]

As depicted in Figure 1, both reaction pathways utilize amine functionalization of the PDMS surface through plasma treatment designed to generate hydroxyl groups and coupling to 3-aminopropyltriethoxysilane (APTES)[15] [hydroxyl group formation was also achieved without plasma treatment through incubation of PDMS in concentrated NaOH[22] (Figure S2 of the Supporting Information)]. While one approach starts with amine derivatization of a planar PDMS building block (Figure 1, top pathway), in another scheme we initially created a wrinkled surface morphology (Figure 1, bottom pathway). Wrinkled PDMS surfaces were prepared by mechanical stretching and release combined with UVO exposure, resulting in formation of a regularly spaced, wavy surface morphology.[14] The two types of amine-functionalized PDMS surfaces were incubated with $Au(SCN)_4^-$ in aqueous acidic solutions at 4 °C,

resulting in coating of the PDMS with metallic gold. Recent studies indicate that formation of gold layers occurs through electrostatic attraction of the $Au(SCN)_4^-$ complex to the amine residues displayed on the surface and subsequent reduction and crystallization of the Au ions without co-addition of reducing agents.[12,13] The gold coating step was followed by a brief incubation with a PEDOT/PSS solution, producing an electrically conductive coating on the PDMS surface. Bending of the Au-coated planar PDMS was subsequently conducted (Figure 1, middle right), which was designed to assess whether conductivity could be retained following mechanical modification of the coated surface.

Figure 2 presents scanning electron microscope (SEM) images of the different PDMS surfaces following deposition of

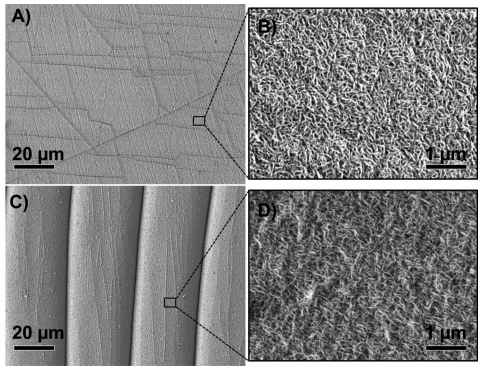

Figure 2. Surface morphology of Au-coated PDMS. Scanning electron microscopy (SEM) images of a Au-coated planar PDMS surface (A and B) and a Au-coated wrinkled PDMS (C and D).

the gold layers. The SEM images in panels A and C underscore the uniform gold coverage of both the planar PDMS surface and the wrinkled surface, respectively. The SEM results also depict interspersed horizontal "grooves" on the PDMS surfaces, previously observed and ascribed to intrinsic stress within the polymer matrix and grain boundary formation.[23,24] Closer examination of the surface reveals a dense "nanoribbon" morphology of the gold films (Figure 2B,D), similar to films produced upon incubation of $Au(SCN)_4^-$ with amine-modified glass surfaces.[12] The predominant presence of gold within the films imaged in Figure 2 was confirmed with energy-dispersive X-ray spectroscopy (EDS) analysis (Figure S3 of the Supporting Information). Importantly, control experiments verified that amine modification of PDMS had a critical role in affecting formation of the nanostructured gold films. Figure S4 of the Supporting Information, for example, demonstrates that Au films were absent when PDMS was not pretreated with APTES (and thus not displaying amine residues). Atomic force microscopy (AFM) analysis implied a thickness of approximately 300 nm of the gold film deposited on the PDMS surface with a roughness of 40 ± 5 nm (Figure S5 of the Supporting Information).

The direct relationship between amine display and Au deposition provides a readily applied route for surface patterning. Figure 3, for example, depicts gold patterns formed on PDMS through the localized display of amine moieties. As outlined in Figure 3A, a stainless steel shadow mask with a desired pattern was placed over APTES-modified PDMS substrates and was subjected to plasma treatment, which removed the amine residues from the exposed areas. Following incubation with $Au(SCN)_4^-$, gold patterns were apparent upon the PDMS surface, essentially tracing the amine-displaying areas.

Elucidating the chemical species and crystalline properties of the Au films grown at the PDMS surface was conducted via application of XPS and powder X-ray diffraction (XRD) (Figure 4). The XPS spectrum in Figure 4A shows two peaks

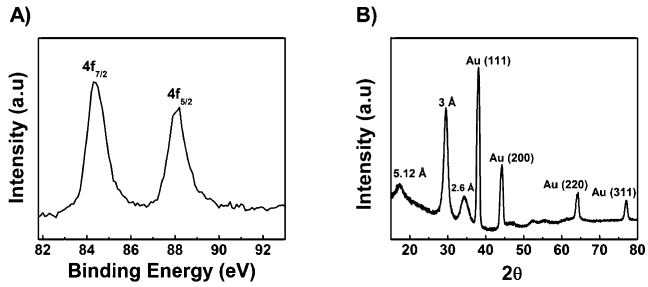

Figure 4. Structural characterization of the Au films grown on PDMS. (A) XPS spectra in the Au (4f) region. (B) XRD pattern.

corresponding to binding energies of 88.2 and 84.3 eV, ascribed to the $4f_{5/2}$ and $4f_{7/2}$ peaks of Au(0), respectively. This result confirms that the Au film predominantly comprises Au(0). The

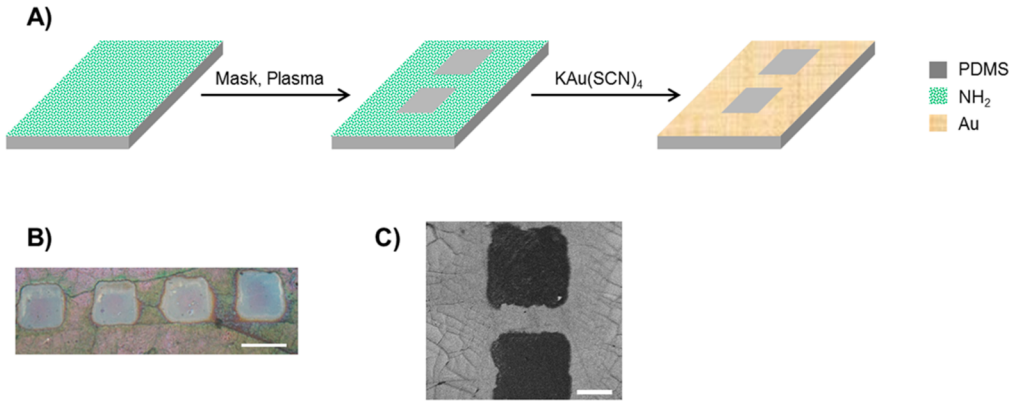

Figure 3. Au patterning on PDMS. (A) Schematic representation of the patterning process through selective etching of the NH_2 regions. Gray color denotes PDMS, green color the amine-modified PDMS surface, and textured yellow color the Au film. (B) Optical microscope image of a patterned surface. The areas within the squares are devoid of Au. The scale bar corresponds to 100 μm. (C) SEM image of a patterned surface. The dark areas are devoid of Au. The scale bar corresponds to 50 μm.

dx.doi.org/10.1021/am4053656 | ACS Appl. Mater. Interfaces 2014, 6, 3341−3346

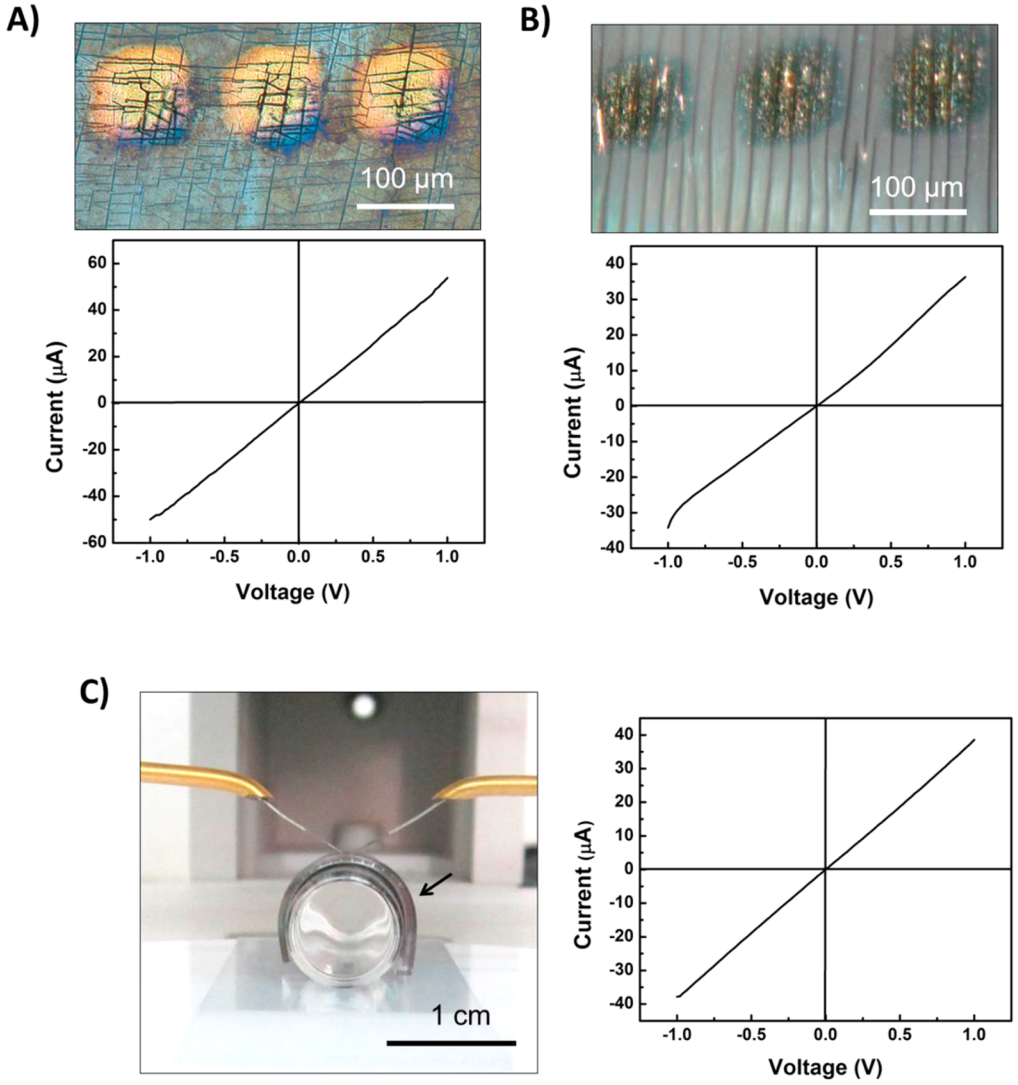

Figure 5. Electrical conductivity in different PDMS surface morphologies. (A) Planar PDMS. Optical microscopy image of the electrode configuration (picture showing three bright square electrodes deposited on the surface) (top) and the corresponding *I*–*V* curve (bottom). (B) Wrinkled PDMS. Optical microscopy image of the electrode configuration (picture showing three square electrodes) (top) and the corresponding *I*–*V* curve (bottom). (C) Physical bending of coated PDMS. Picture of the experimental setup, showing the two electrodes in contact with the bent PDMS (the arrow points to the PDMS slab wrapped around a glass tube) (left), and the corresponding *I*–*V* curve (right). The Ohmic (linear) behavior apparent in all *I*–*V* curves indicates electrical conductivity.

XRD pattern in Figure 4B highlights the crystallinity of the metallic Au(0) film, showing signals ascribed to Au(111), Au(200), Au(220), and Au(311) crystal planes. Additional peaks at 5.12, 3, and 2.6 Å are assigned to $Au(SCN)_2^-$ crystallites formed through *aurophilic* interactions.[12,25] XPS and XRD analyses performed on Au films grown over the wrinkled PDMS surface gave similar results (Figure S6 of the Supporting Information). Together, the XPS and XRD data in Figure 4 verify that the self-assembled films grown at the amine-derivatized PDMS surfaces mostly comprise metallic, crystalline gold.

The goal of this study is the fabrication of conductive layers deposited on PDMS in nonplanar configurations. Figure 5 presents the conductivity profiles of PDMS surfaces prepared through the processes shown in Figure 1. The linear current–voltage (*I*–*V*) curves recorded for the different surface morphologies in Figure 5 underscore the significant electrical conductivity attained by the new film fabrication technology for the planar and nonplanar surfaces. It should be noted that PEDOT/PSS spin coating was conducted following gold deposition to enhance electron transport within the Au films. Addition of a PEDOT/PSS solution gave rise to higher conductivity, likely by filling the grooves on the Au/PDMS surface (which are apparent in the SEM images in Figure 2), as well as through "nanosoldering" of the interspersed Au nanoribbons,[26] overall eliminating possible gaps in electron transport.

Figure 5A (top) presents an optical microscopy image of the experimental setup for measuring conductivity in the planar Au/PEDOT/PSS/PDMS surface configuration, showing the square-shaped gold electrode pads deposited on the coated PDMS surface. The linear *I*–*V* curve recorded between adjacent electrodes corresponding to a spacing of approximately 50 μm (Figure 5A, bottom graph) indicates Ohmic behavior and a reasonably good sheet resistance of 6×10^3 Ω/square. A remarkable conductivity profile was apparent for the wrinkled PDMS surface (Figure 5B). The optical image in Figure 5B demonstrates that conductivity was measured over

several "ridges" between adjacent electrode pads. Indeed, the $I-V$ curve in Figure 5B demonstrates that electrical conductivity was retained even in this nonplanar surface morphology. The wrinkled Au/PDMS sheet resistance of 14×10^3 Ω/square is on the same order of magnitude as the value obtained for the planar Au/PDMS surface (Figure 5A), recorded with larger electrode spacings, underscoring the ability of the new approach to achieve effective coating of three-dimensional objects with a conductive layer. Notably, the planar PDMS sample was conductive with electrode spacings of up to 500 μm, while the wrinkled surfaces exhibited conductivity with an up to 1 mm electrode separation (Figure S7 of the Supporting Information). This might be related to a more uniform Au film formed upon a wrinkled surface, because of the higher hydrophilicity and lower abundance of cracks. Indeed, it has been reported that small protrusions can be formed during plasma treatment of planar PDMS, because of lattice mismatch between the oxidized top layer and native interior.[21,24] This might result in an uneven surface and the occurrence of defects in the metallic films grown over it, which could adversely affect electron transport. Such lattice mismatch-induced surface deformations are not expected to occur upon plasma treatment of wrinkled PDMS because the surface is already oxidized through ozone treatment.

To further test the feasibility of the technology for achieving conductivity in flexible, bent surface configurations, we examined the effect of mechanical modification of surface curvature (Figure 5C). As shown in the photograph in Figure 5C, the flat Au-coated PDMS slab (complemented with PEDOT/PSS surface treatment) was bent around a small-diameter glass tube and the conductivity was measured between two electrodes placed upon the bent PDMS surface. The $I-V$ curve in Figure 5C clearly demonstrates that even in the bent configuration (~2.2 cm^{-1} curvature) the coated PDMS retained its conductivity. Indeed, the sheet resistance measured, 8×10^3 Ω/square, was comparable to the value recorded in the initial, planar configuration.

The gold-coated polymer substrates were resilient and durable. Both planar and wrinkled polymer systems (Figure 2) were stable under ambient conditions and were found to retain their electrical conductivity even when the systems were tested after several months. Similarly, the conductivity of the bent PDMS film (sample shown in Figure 5C) was hardly diminished even after a long period of time. Following mechanical cycling (bending and/or straightening), however, the conductivity was gradually lost, likely because of the disruption of film continuity and blocked macroscopic electrical contacts.

It also should be emphasized that conductivity in all cases was dependent both upon deposition of the Au film on the PDMS surface and PEDOT/PSS treatment, as shown in Figure 1. Specifically, control experiments demonstrated that PDMS or amine-modified PDMS that was not incubated with the Au thiocyanate complex was not conductive even after spin coating with a PEDOT/PSS solution. Similarly, no conductivity was recorded for PDMS substrates coated with nanostructured gold, but not subsequently treated with a PEDOT/PSS solution.

CONCLUSIONS

This paper describes a simple yet seemingly powerful method for assembling conductive, patterned films upon both planar and nonplanar PDMS surfaces. The technology employs amine functionalization of the polymer surface followed by incubation with $Au(SCN)_4^-$ (without co-addition of any reducing agents). The nanostructured Au film formed upon the PDMS surface was further treated with a PEDOT/PSS solution to enhance the conductivity. We demonstrate that the technology can be successfully implemented in varied surface morphologies giving rise to electrically conductive surface layers; importantly, conductivity was retained even upon physical deformation of coated PDMS.

While currently employed top-down technologies such as lithography demonstrate excellent patterning capabilities and conductivity profiles, the experimental approach outlined here exhibits notable favorable characteristics for practical applications in nonplanar conductive films. Gold coating is conducted in an aqueous solution, under mild conditions of temperature and pressure, using inexpensive and nontoxic reagents. The technology can be easily scaled to mass production applications, and pattern formation is an intrinsic outcome of the synthetic route. This generic bottom-up synthetic approach could be broadly applied for the fabrication of conductive flexible surfaces in two and three dimensions and contribute to a range of practical applications.

ASSOCIATED CONTENT

Supporting Information

Photograph of the mechanical stretching device, SEM images of samples obtained after NaOH treatment of PDMS, EDS analysis of the Au–PDMS substrates, SEM results of a control experiment without amine modification of PDMS, AFM analysis of Au–PDMS substrates, XPS and XRD analyses of gold-wrinkled PDMS samples, and $I-V$ curves for samples with larger electrode separations. This material is available free of charge via the Internet at http://pubs.acs.org.

AUTHOR INFORMATION

Corresponding Author

*E-mail: razj@bgu.ac.il.

Notes

The authors declare no competing financial interest.

ACKNOWLEDGMENTS

We thank Dr. Dimitry Mogiliansky for XRD measurements, Dr. Natalya Froumin for XPS measurements, and Dr. Jurgen Jopp for AFM analysis. This work was partially supported by an Infrastructure Grant of the Ministry of Science and Technology (MoST).

REFERENCES

(1) Cheng, I.-C.; Wagner, S. Overview of Flexible Electronics Technology. In *Flexible Electronics: Materials and Applications*; Wong, W. S., Salleo, A., Eds; Springer: New York, 2009; pp 1–28.

(2) Nathan, A.; Ahnood, A.; Cole, M. T.; Lee, S.; Suzuki, Y.; Hiralal, P.; Bonaccorso, F.; Hasan, T.; Garcia-Gancedo, L.; Dyadyusha, A.; Haque, S.; Andrew, P.; Hofmann, S.; Moultrie, J.; Chu, D.; Flewitt, A. J.; Ferrari, A. C.; Kelly, M. J.; Robertson, J.; Amaratunga, G. A. J.; Milne, W. I. *Proc. IEEE* **2012**, *100*, 1486–1517.

(3) Sun, D. M.; Liu, C.; Ren, W. C.; Cheng, H. M. *Small* **2013**, *9*, 1188–1205.

(4) Tobjörk, D.; Österbacka, R. *Adv. Mater.* **2011**, *23*, 1935–1961.

(5) Rogers, J. A.; Someya, T.; Huang, Y. *Science* **2010**, *327*, 1603–1607.

(6) Long, Y. Z.; Yu, M.; Sun, B.; Gu, C. Z.; Fan, Z. *Chem. Soc. Rev.* **2012**, *41*, 4560–4580.

(7) Wong, W. S.; Chabinyc, M. L.; Ng, T.-N.; Salleo, A. Materials and Novel Patterning methods for Flexible Electronics. In *Flexible Electronics: Materials and Applications*; Wong, W. S., Salleo, A., Eds; Springer: New York, 2009; pp 143−182.
(8) Kim, J.-H.; Hong, S. H.; Seong, K.-d.; Seo, S. *Adv. Funct. Mater.* **2013**, DOI: 10.1002/adfm.201303478.
(9) Talapin, D. V.; Lee, J.-S.; Kovalenko, M. V.; Shevchenko, E. V. *Chem. Rev.* **2010**, *110*, 389−458.
(10) Lu, W.; Lieber, C. M. *Nat. Mater.* **2007**, *6*, 841−850.
(11) Bai, C.; Liu, M. *Nano Today* **2012**, *7*, 258−281.
(12) Morag, A.; Froumin, N.; Mogiliansky, D.; Ezersky, V.; Beilis, E.; Richter, S.; Jelinek, R. *Adv. Funct. Mater.* **2013**, *23*, 5663−5668.
(13) Vinod, T. P.; Zarzhitsky, S.; Morag, A.; Zeiri, L.; Levi-Kalisman, Y.; Rapaport, H.; Jelinek, R. *Nanoscale* **2013**, *5*, 10487−10493.
(14) Lee, S. G.; Kim, H.; Choi, H. H.; Bong, H.; Park, Y. D.; Lee, W. H.; Cho, K. *Adv. Mater.* **2013**, *25*, 2162−2166.
(15) Roth, J.; Albrecht, V.; Nitschke, M.; Bellmann, C.; Simons, F.; Zschoche, S.; Michel, S.; Luhmann, C.; Grundke, K.; Voit, B. *Langmuir* **2008**, *24*, 12603−12611.
(16) McDonald, J. C.; Whitesides, G. M. *Acc. Chem. Res.* **2002**, *35*, 491−499.
(17) Seethapathy, S.; Górecki, T. *Anal. Chim. Acta* **2012**, *750*, 48−62.
(18) Bai, H. J.; Shao, M. L.; Gou, H. L.; Xu, J. J.; Chen, H. Y. *Langmuir* **2009**, *25*, 10402−10407.
(19) Wu, W. Y.; Zhong, X.; Wang, W.; Miao, Q.; Zhu, J. J. *Electrochem. Commun.* **2010**, *12*, 1600−1604.
(20) Moon, G. D.; Lim, G. H.; Song, J. H.; Shin, M.; Yu, T.; Lim, B.; Jeong, U. *Adv. Mater.* **2013**, *25*, 2707−2712.
(21) Bowden, N.; Brittain, S.; Evans, A. G.; Hutchinson, J. W.; Whitesides, G. M. *Nature* **1998**, *393*, 146−149.
(22) Slentz, B. E.; Penner, N. A.; Lugowska, E.; Regnier, F. *Electrophoresis* **2001**, *22*, 3736−3743.
(23) Akogwu, O.; Kwabi, D.; Midturi, S.; Eleruja, M.; Babatope, B.; Soboyejo, W. O. *Mater. Sci. Eng., B* **2010**, *170*, 32−40.
(24) Graudejus, O.; Görrn, P.; Wagner, S. *ACS Appl. Mater. Interfaces* **2010**, *2*, 1927−1933.
(25) Schmidbaur, H. *Gold Bull.* **2000**, *33*, 3−10.
(26) Lee, J.; Lee, P.; Lee, H. B.; Hong, S.; Lee, I.; Yeo, J.; Lee, S. S.; Kim, T. S.; Lee, D.; Ko, S. H. *Adv. Funct. Mater.* **2013**, *23*, 4171−4176.